octahedron, and both these values are significantly less than 3·81 Å, the ideal S–S distance. On the other hand, all the S–S distances in both types of tetrahedron are greater than 3·81 Å, the average values being 4·01 Å for an In3–S tetrahedron and 4·04 Å for a vacant tetrahedron.

Table 3. *Bond lengths*

Standard deviation in each bond length = 0·01 Å

		Å
In1–S Octahedron		
	In–S1(1), In–S1(2)	2·68
	In–S2(2)	2·54
	S1(1)–S1(2)	3·76
	S1(1)–S1(4)	3·81
	S1(1)–S2(2), S1(2)–S2(2)	3·64
	S1(3)–S2(2), S1(4)–S2(2)	3·74
In2–S Octahedron		
	In–S2(1), In–S2(2)	2·56
	In–S3(1), In–S3(2)	2·68
	In–S3(4)	2·63
	In–S1(1)	2·65
	S1(1)–S2(1), S1(1)–S2(2)	3·64
	S1(1)–S3(1), S1(1)–S3(2)	3·81
	S2(1)–S3(1), S2(2)–S3(2)	3·82
	S2(1)–S2(2)	3·68
	S3(1)–S3(2)	3·45
	S2(1)–S3(4), S2(2)–S3(4)	3·90
	S3(1)–S3(4), S3(2)–S3(4)	3·47
In3–S Tetrahedron		
	In–S1(4), In–S1(5)	2·44
	In–S3(2), In–S3(3)	2·48
	S1(4)–S1(5)	3·86
	S1(4)–S3(2), S1(4)–S3(3) ⎫ S1(5)–S3(2), S1(5)–S3(3) ⎭	4·01
	S3(2)–S3(3)	4·17
Vacant tetrahedron		
	S2(1)–S2(3), S2(4)–S2(5)	3·94
	S2(2)–S2(4), S2(2)–S2(5) ⎫ S2(3)–S2(4), S2(3)–S2(5) ⎭	4·10

See Fig. 1 for location of atoms.

We wish to thank Dr P. J. Wheatley, of Monsanto Research S.A., for providing computer programs which have been used in this work.

References

BOND, W. L. (1959). *Acta Cryst.* **12**, 375.
DALY, J. J., STEPHENS, F. S. & WHEATLEY, P. J. (1963). M.R.S.A. Final Report No. 52.
GOODYEAR, J. & STEIGMANN, G. A. (1961). *Proc. Phys. Soc.* **78**, 491.
KING, G. S. D. (1962). *Acta Cryst.* **15**, 512.
PHILLIPS, D. C. (1954). *Acta Cryst.* **7**, 746.
ROOYMANS, C. J. M. (1959). *J. Inorg. Nucl. Chem.* **11**, 78.
WILSON, A. J. C. (1960). *X-ray Diffraction by Polycrystalline Materials.* London: Institute of Physics.

Acta Cryst. (1965). **19**, 971

Oxygen Coordinates of Compounds with Garnet Structure*

BY FERDINAND EULER AND JANE A. BRUCE

Air Force Cambridge Research Laboratories, Office of Aerospace Research, Bedford, Massachusetts, U.S.A.

(*Received* 23 *May* 1963, *and in revised form* 19 *April* 1965)

By full-matrix least-squares refinement, the O parameters of one natural and twelve synthetic garnets $M_5R_3O_{12}$ were determined, with M and R as follows:

M:	Al	Ga	Fe .....
R:	Lu Yb Y Gd	Lu Yb Y	Lu Yb Y Dy Sm .

The refinement was based on those Bragg reflections to which only the oxygen ions contribute. The integrated X-ray intensities were counted after elimination of Renninger effects. The resulting O parameters are interpreted by polar coordinates which indicate size, shape and orientation of the oxygen octahedra and are closely associated with the effects of shortened shared edges on the shape of the other polyhedra. The cell edges *a* are studied as functions of the rare-earth atomic numbers. The crystal field effects on *a*, shown by Espinosa on iron garnets with non-spherical ions R, appear also in the other two series. For spherical R, the increments Δa associated with changes in M and R are independent of each other. Such additivity of *a* is destroyed in $Al_5Gd_3O_{12}$ by the resistance of the large rare-earth ions to the small lattice. These effects are demonstrated also on selected interionic distances and angles.

Introduction

As Menzer (1928) has found, the garnet structure belongs to the space group $Ia3d(O_h^{10})$ with cations in 16(*a*), 24(*c*) and 24(*d*) positions,* defined by fixed fractions of the cubic cell edge *a*. The 96(*h*) positions of the anions (oxygen in most garnets) depend on three variable structure parameters *x*, *y*, *z* which, in general, differ with composition.

* Portions of this work were presented at the Pittsburgh Diffraction Conference, Pittsburgh, Pennsylvania, on November 7, 1962.

* Nomenclature of *International Tables for X-Ray Crystallography* (1952).

Geller & Gilleo (1957, 1959) and, recently, Batt & Post (1962) have determined these parameters for $Y_3Fe_5O_{12}$ (YIG),† Prince (1957) for YAlG, Abrahams & Geller (1958) for $Ca_3Al_2Si_3O_{12}$ (grossularite) and Weidenborner (1961) for GdIG. In view of the current interest in crystal field effects in rare-earth garnets of the Al, Ga and Fe series, it was found necessary to obtain a larger variety of these parameters. Therefore, we determined these on twelve additional garnet compounds as reported in the following.

Experiments and computations

The single-crystal samples used in this work were grown from the melt with PbO and PbO–PbF_2 fluxes at these Laboratories (Pitha, Moriarty), Hughes Research Laboratories, Malibu, California (Lefever), Westinghouse Research Laboratories, Pittsburgh, Pennsylvania (Bailey) and the Clarendon Laboratory, Oxford, England (Garton) as shown in Tables 1 and 4 by the letters *P*, *M*, *L*, *B* or *G*. The mineral sample was obtained from the Adirondacks Museum, Blue Mountain Lake, N.Y. Its composition was determined to be $\{Mg_{1\cdot6}Fe_{1\cdot2}Ca_{0\cdot2}\}$ $[Al_2]$ $(Si_3)O_{12}$, with the different brackets indicating (*c*), (*a*) and (*d*) sites.

The lattice constants *a* were determined from Debye–Scherrer photographs. Of each compound, one crystal was then selected for the intensity measurements required to obtain *x*, *y*, and *z*. With the use of an air cyclone grinder similar to that described by Bond (1951), it was ground into a sphere of approximately ½ mm diameter and mounted on a Weissenberg goniometer. Iron-filtered Co $K\alpha$ radiation was used, except for SmIG for which Fe $K\alpha$ was chosen. The diffracted X-rays were detected with a stationary Geiger counter, NORELCO scaler and ratemeter, while the sample was oscillated through the reflecting positions. Sufficient counts were obtained for 3% statistical error of the net intensities. Sample orientation was kept within 0·03° of the [110] oscillation axis ([001] with YAlG, YbGaG, LuIG(*M*) and DyIG.

Uncertainties about cation scattering factors and dispersion were reduced by the selection of those reflections to which only the anions contribute. These are generally weak and consequently liable to substantial intensity increase from simultaneous reflections (Renninger, 1937) as found in approximately one out of five cases, although systematic effects such as reported by Yakel & Fankuchen (1962) were absent here. Owing to the large cell edge *a*, the possibilities for simultaneous reflections are numerous and defy quick theoretical prediction. Therefore, each reflection was examined by rotating the crystal in the plane of reflection about a few degrees. Owing to the Weissenberg geometry, this had to be done in the following three steps:

(1) Rotate about the vertical axis by 1, 2 or 3° from equi-inclination setting;
(2) Reset the counter tube accordingly;
(3) Rotate about the horizontal axis for maximum counting rate. This maximum must be independent of the setting if simultaneous reflections are to be avoided.

The net intensities were corrected by Lorentz-polarization, Tunell (1939) and absorption factors, the latter as tabulated by Bond (1959). The resulting structure amplitudes $|F_o|$'s were divided into three groups: measured, estimated* and unobserved, and were weighted as shown in Table 1. The scale factor *s*, the three structure parameters *x*, *y* and *z* and the oxygen temperature factor B_h were refined by the full-matrix least-squares method, starting with the parameters obtained for YIG by Geller & Gilleo (1957, 1959).

For the computations, both IBM 704 and 7090 computers were used with the programs by Busing & Levy (1959, 1962). The atomic scattering factors for O^{2-} were based on the tables by Freeman (1959).

During the first three or four refinement cycles, B_h was kept constant. Then all five parameters were refined simultaneously until no significant changes of *x*, *y*, and *z* were indicated. Zero parameter changes could be maintained through three to six cycles, and no case of increasing weighted *r* was observed.

With the aid of the Busing, Martin & Levy (1964) FORTRAN Function and Error program, the interionic distances d_i were computed on an IBM 7090. The subscripts *i* refer to the number of nearest anions to the (*d*), (*a*) or (*c*) sites as shown in Fig. 1. In addition, all

* With statistical counting error larger than 3%.

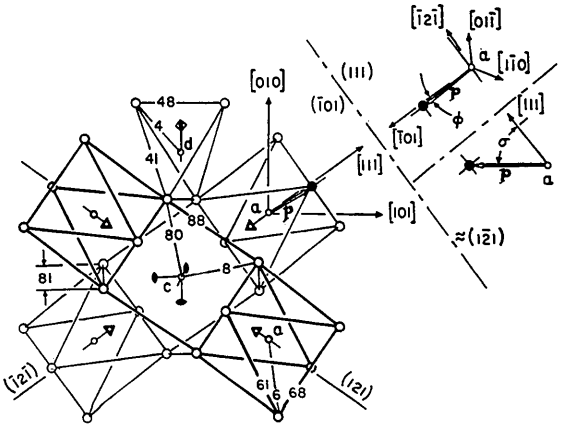

Fig. 1. Arrangement of the anion polyhedra (CN 4, 6, 8) in garnets, $(\bar{1}01)$ projection; cation sites (*d*), (*a*), (*c*); point symmetries $\bar{4}$, $\bar{3}$ and 222. Interionic distances d_i (*i*: 4, 6, 8, 80; 41, 61, 81; 48, 68, 88; the last three pertain to shared edges of neighboring polyhedra). Cell origin at *a* site (intersection of [010] and [101]); vector **p**, pointing from there to anion position *x*, *y*, *z* (solid circle), is specified by magnitude *p*, angles σ and φ, shown in projections $\sim(12\bar{1})$ and (111). The octahedra are regular if $\sigma=\sigma_0=\cos^{-1}(1/\sqrt{3})=54{\cdot}75°$. Right trigonal prisms are found between two octahedra if $\varphi=0$, associated with degenerate dodecahedra bound by two parallel rectangles ($d_8=d_{80}$); their most degenerate form ($d_{88}=d_{68}=d_{61}$ and $d_{48}=d_{81}$) requires, in addition, $p=0{\cdot}1686$. The tetrahedra are regular if $p=0{\cdot}1470$ (with $\sigma=\sigma_0$ and $\varphi=0$).

† In this paper, the synthetic garnets are identified by the abbreviation RMG with chemical symbols for R and M inserted (except I for iron).

Table 1. *Observed and calculated structure amplitudes F of garnets* $M_5R_3O_{12}$

Scale factor s, oxygen temperature factor B_h and weighted residual $r=[\Sigma w(F_o-F_c)^2\Sigma w\,.\,F_o^2]^{\frac{1}{2}}$ where $w=1/\varepsilon^2$; the standard deviation ε of each F_o is indicated only for the group of estimated F_o; $\varepsilon=1/s$ for measured F_o; $\varepsilon=F_o=F_{min}/2$ for unobserved reflections with F_{min}, shown here, derived from net peak intensity equal to 10 counts sec.$^{-1}$.

M R	Si, Al Mg, Fe, Ca		Al Lu		Al Yb		Al Y		Al Gd		Ga Lu		Ga Yb		Ga Y		Fe Lu (M)		Fe Lu (B)		Fe Yb		Fe Y		Fe Dy		Fe Sm	
s	0.83±0.03		1.40±0.04		1.91±0.06		1.04±0.02		1.38±0.04		1.39±0.05		1.50±0.05		1.53±0.02		1.48±0.07		1.99±0.07		1.80±0.03		0.91±0.02		1.45±0.03		1.00±0.02	
B_h(Å^2)	0.54±0.22		0.30±0.16		0.30±0.19		0.46±0.14		0.18±0.16		0.50±0.21		0.55±0.19		0.37±0.10		0.63±0.32		0.35±0.20		0.93±0.11		0.66±0.13		0.59±0.14		0.61±0.15	
r	0.067		0.046		0.052		0.039		0.045		0.065		0.052		0.026		0.087		0.061		0.033		0.034		0.034		0.038	
h k ℓ	$\|F_o\|$	F_c	$\|F_o\|$	F_c	$\|F_o\|$	F_c	$\|F_o\|$	F_c	$\|F_o\|$	F_c	$\|F_o\|$	F_c	$\|F_o\|$	F_c	$\|F_o\|$	F_c	$\|F_o\|$	F_c	$\|F_o\|$	F_c	$\|F_o\|$	F_c	$\|F_o\|$	F_c	$\|F_o\|$	F_c	$\|F_o\|$	F_c
0 8 2	45	42	69	67	70	66	60	59	61	59	92	85	87	82	81	79	90	87	95	88	81	78	84	79	83	80	80	75
0 8 6	16	− 9	<17	−10	15±4	− 8	11±4	−6	<10	−4	<19	−14	<17	−17	< 9	−10	<18	−20	18	−17	<11	−12	<15	−11			<18	−9
0 8 10									25	25	38	38									32	31						
2 4 12											12±2	−6							15±1	−4	11±1	−4						
2 6 10	35	33	51	52	49	51	45	45	44	46	61	62	60	60	59	59	59	61	60	64	54	54	55	56	59	58	54	55
4 1 3	111	113	111	112	110	111	111	112	113	114	102	107	106	109	109	110	106	109	106	110	106	107	108	110	109	111	110	112
4 1 5	16	17	26±4	24	26±4	23	20±3	20	25	20	40±4	27	27	27	28	27	26	30	36±3	30	29±2	27	<20	27	28	28	28±5	26
4 1 7	67	63	56	55	58	56	60	57	60	58	50	49	51	52	53	52	49	47	46	48	49	48	50	49	54	51	52	53
4 1 9	73	79	78	77	79	79	80	80	87	86	65	64	65	65	74	72	61	57	63	62	64	63	68	67	70	68	76	74
4 1 11	41	−39	37	−34	37	−34	34	−34	37	−36	35	−26	30	−29	31	−31	31	−28	33	−29	29	−26	33	−29	32	−31	34	−31
4 3 5	29	−24	<21	−18	26±4	−20	<14	−24	32±2	−29	<23	−6	<20	−5	<10	−14	<20	−1	<18	−4	<13	−9	<20	−12	<17	−11	<24	−16
4 3 7	34	−34	46	−45	42	−45	44	−43	44	−45	48	−48	47	−47	49	−49	55	−50	51	−52	47	−47	48	−49	49	−49	46	−48
4 3 9	40	−42	45	−47	44	−46	43	−42	43	−43	45	−46	47	−47	47	−48	51	−51	52	−52	45	−45	47	−48	50	−50	45	−48
4 3 11	10	−13	28	−25	24	−23	15	−18	18	−15	30	−36	31	−36	30	−31	35	−40	38	−40	28	−31	30	−31	29	−33	25	−28
4 5 7	67	66	70	73	71	72	68	69	70	71	73	73	77	74	75	75	72	73	76	76	69	69	74	73	76	74	74	74
4 5 9	11	12	18±3	−5	13±3	−5	15±3	−2	8±2	−4	16±4	−13	<15	−9	22±7	−12	16	−12	14±3	−14	< 9	−11	<13	−11	<12	−10	<14	−9
4 5 11			11±2	−7	16±1	−7			11	−10	12±2	−8							11±2	−9	8±1	−8	< 9	−9				
4 7 9	21	−20	14±2	−10	15±2	−9	11±2	−8	< 6	−7	<12	−5	13	−8	9	−7	20	−11	14±2	−10	< 7	−6			8±3	−9	11	−8
8 1 3	10±2	−10	<20	−16	21±4	−14	15±3	−10	<12	−8	22±5	−24	23	−24	20	−20	32	−30	31±2	−29	22±2	−22	<17	−22	24	−23	<22	−18
8 1 5	64	−62	66	−63	67	−63	65	−63	65	−65	62	−58	61	−59	63	−62	57	−56	65	−59	58	−56	60	−59	61	−61	63	−62
8 1 7	18	−14	32	−27	33	−26	26	−23	31	−25	36	−33	36	−31	35	−32	37	−33	38	−35	32	−30	33	−32	34	−32	33	−30
8 1 9	44	42	55	57	55	57	53	54	57	58	57	59	55	56	60	61	55	57	59	62	52	54	56	58	56	58	57	58
8 3 5	87	−89	91	−93	91	−95	91	−94	97	−99	87	−90	88	−91	90	−93	82	−85	88	−89	82	−84	86	−88	86	−89	92	−92
8 3 7	42	−39	29±2	−21	28	−25	33	−31	40	−35	17±4	−4	<15	−7	< 8	−11	12	6	11±4	4	< 9	− 5	<13	− 6	<12	− 6	16±3	−14
8 3 9	21	−20	15±2	−14			20	−19	20	−19	9±3	−10	15	−11	12	−11	15	− 2			8±1	− 8	<11	− 7	< 8	− 7	9±6	−11
8 5 7	21	20	16±2	11	15±2	12	< 8	13	16	16	<13	2	<12	3	< 7	7	<12	2	21±2	3	< 8	4	<11	6	<10	7	<12	9
8 5 9											22	−24							24	−25	22	−23						
12 1 3	30	35	48	49	48	49	45	47	49	51	49	52	46	49	53	53	43	47	52	53	46	46	49	49	49	49	48	50
12 1 5																			18	13								

bond angles with vertices at the (h) site and finally, the polar coordinates p, σ and φ of the vector **p** (shown in Fig. 1) were also computed. The latter are defined by the equations

$$p^2=x^2+y^2+z^2 \quad (1)$$

$$\cos\sigma=(x+y+z)/(\sqrt{3}p) \quad (2)$$

$$\sin\varphi=(x+z-2y)/(\sqrt{6}p\sin\sigma) \quad (3)$$

and indicate size, shape and orientation of the anion octahedra.

Results

The observed and calculated structure amplitudes are presented in Table 1, which shows also the refined parameters s and B_h and the weighted residual r. At first, a few reflections yielded exceptionally large differences $|F_o|-|F_c|$ listed in Table 2. These are always positive, hinting that the effect of simultaneous reflections was not fully eliminated in these cases. Therefore, the refinement was repeated with F_o and ε changed as indicated and the result shown in Table 1. It produced

Table 2. *Reflections yielding large differences* F_o-F_c *after the first refinement*

M	R	h	k	l	s	$\|F_o\|$	F_c	Changes
Al	Y	4	5	9	1·04	15±2	− 3	ε
Al	Gd	4	5	9	1·40	18	− 8	F_o, ε
Ga	Y	4	5	9	1·58	42	−20	F_o, ε
Fe	Yb	2	4	12	1·80	11	− 4	ε
Fe	Sm	4	7	9	0·98	21	−11	F_o

Table 3. *Correlation matrices resulting from refinement of scale factor s, structure parameters x, y, and z, and oxygen temperature factor* B_h *in garnets* $M_5R_3O_{12}$

The matrix elements a_{ij} were multiplied by 100, diagonal elements $a_{ii}=1$ omitted. The figures for GdIG are based on Weidenborner's (1961) F_o.

M:	Si, Al	Al				Ga				Fe			
R	12 -5 -7 91 2 -6 14 4 -5												
Mg, Fe, Ca:	-1		x	y	z	B_h							
Lu:		s	18	3	-27	91	18	3	-39	92	14	7	-34 91
		x		-21	-4	24		-15	-6	23		-10	-15 16
		y			3	3			8	1			2 -1
		z				-17				-32		(B)	-26
Yb:			19	-1	-29	91	16	3	-29	91	19	2	-38 92
				-35	-8	24		0	1	21		-12	-7 24
					1	-3			-14	1			9 5
						-18				-19			-30
Y:			22	-6	-26	91	17	3	-27	91	20	3	-32 91
				-26	-7	28		2	2	23		-19	-9 25
					3	-8			-14	1			5 0
						-13				-13			-20
Dy:											19	3	-33 91
												-19	-6 25
													-13 -1
													-22
Gd:			24	-8	-28	91					24	0	-37 88
				-24	-15	28						13	-12 6
					10	-8							30 -2
						-19							-28
Sm:											14	8	-24 91
												-18	9 21
													-8 6
													-11

Table 4. *Structure data of garnets*

See text for composition of mineral garnet and origin code, Fig. 1 for definition of polar coordinates and interatomic distances. Cell edges *a* of YbIG and DyIG from Espinosa (1962).

M (3 in d, 2 in a)	Si, Al	Al	Al	Al	Al	Ga	Ga	Ga	Fe	Fe	Fe	Fe	Fe	Fe
R (3 in c)	Mg_3Fe_2Ca	Lu	Yb	Y	Gd	Lu	Yb	Y	Lu	Lu	Yb	Y	Dy	Sm
in garnet $M_5R_3O_{12}$														
Origin code	mineral	G	G	L	G	G	L	L	M	B	P	P	P	P
• Oxygen parameters														
-10^4x	339±5	294±4	296±5	306±4	311±4	252±5	259±5	272±2	251±8	255±5	263±3	270±4	272±4	282±4
10^4y	491 6	537 5	529 6	512 4	509 4	570 8	563 5	558 3	595 8	592 8	570 5	569 5	570 5	552 5
10^4z	1535 6	1509 6	1504 7	1500 5	1490 5	1506 8	1519 7	1501 3	1523 10	1514 8	1506 5	1505 5	1511 5	1503 5
• Polar coordinates														
radial 10^4p	1647 6	1628 6	1622 7	1614 5	1605 5	1630 8	1641 7	1624 3	1654 10	1645 8	1632 4	1631 5	1638 5	1626 5
cone angle 10σ(°)	537 2	516 2	518 2	524 1	526 1	498 2	501 2	506 1	493 3	495 2	501 1	503 1	504 1	510 2
azimuth 10φ(°)	38 2	26 2	28 2	31 2	30 2	21 3	25 2	21 1	15 4	14 3	19 2	18 2	18 2	22 2
• Distances in 10^{-3} Å														
cell edge a	11556 4	11906 4	11931 4	12000 4	12113 4	12188 4	12204 4	12280 4	12290 4	12278 4	12302 1	12376 4	12405 1	12540 4
cation-anion														
d-h (tet.) d_4	1635 7	1760 6	1762 8	1761 5	1781 5	1852 9	1835 7	1849 3	1867 11	1868 8	1861 4	1866 5	1864 5	1875 5
a-h (oct.) d_5	1903 7	1939 7	1935 8	1937 6	1944 6	1987 10	2002 8	1995 4	2033 12	2019 10	2007 5	2019 6	2031 6	2039 6
c-h (dod.) 1) d_6	2377 7	2383 6	2397 7	2432 5	2458 5	2393 10	2407 7	2428 3	2385 9	2385 10	2417 5	2434 6	2439 6	2489 6
2) d_{80}	2222 6	2276 6	2283 7	2303 5	2335 5	2303 8	2302 7	2338 3	2319 11	2326 8	2335 4	2356 5	2360 5	2394 5
anion-anion (h-h)														
shared (tet,dod) d_{48}	2502 14	2684 13	2691 16	2696 11	2740 11	2793 19	2761 15	2810 7	2812 23	2826 19	2820 10	2837 12	2832 12	2858 12
(oct,dod) d_{68}	2658 11	2632 11	2633 13	2658 9	2675 8	2626 14	2660 13	2668 6	2671 19	2659 13	2667 7	2692 9	2710 9	2743 9
(dod,dod) d_{88}	2760 15	2750 13	2777 16	2837 11	2889 12	2713 20	2719 15	2786 7	2674 23	2695 19	2754 10	2783 12	2782 12	2865 13
unshared (tet.) d_{41}	2750 11	2964 10	2967 12	2961 9	2988 8	3134 14	3108 11	3117 6	3160 19	3157 13	3142 7	3148 9	3146 9	3159 9
(oct.) d_{61}	2724 13	2848 12	2835 15	2818 10	2821 11	2981 19	2993 14	2966 7	3066 22	3039 18	3001 9	3010 11	3027 11	3017 12
(dod.) d_{81}	2808 11	2877 10	2891 11	2917 8	2936 8	2959 16	2970 13	2965 6	2952 19	2942 16	2968 8	2975 10	2980 9	3022 10
• Bond angles														
in tenth degrees														
a - h - d	1317 4	1282 4	1288 4	1301 3	1307 3	1251 5	1254 4	1265 2	1234 5	1239 5	1255 3	1258 3	1257 3	1271 3
a - h - (d_{80}) - c	1028 2	1040 2	1042 2	1042 2	1042 2	1049 3	1046 3	1045 1	1040 4	1041 3	1045 2	1042 2	1040 2	1042 2
a - h - (d_8) - c	974 3	1002 3	1001 3	997 2	999 2	1017 4	1010 3	1014 1	1018 5	1020 4	1016 2	1015 2	1013 2	1010 2
d - h - (d_{80}) - c	958 3	942 3	941 3	942 2	938 2	937 4	944 3	936 1	938 5	934 4	936 2	935 2	937 2	937 2
d - h - (d_8) - c	1226 3	1226 3	1221 3	1216 2	1213 2	1226 4	1229 4	1225 2	1241 5	1238 4	1229 2	1230 3	1233 3	1226 3
c - h - (d_{80}) - c	1005 3	1029 2	1026 3	1017 2	1014 2	1053 4	1050 3	1042 1	1062 4	1058 3	1049 2	1046 2	1046 2	1037 2

Table 5. *Literature data on structure of garnets* $M_5R_3O_{12}$

Oxygen structure parameters x, y, z and temperature factor B_h; scale factor s; number n_r of all reflections used in the refinement; number n_{ro} of the 'oxygen-only' reflections. Parameters indicated by f were not refined. Sources of observed structure factors F_o, weights w, least-squares refinement program LS and parameters par: *A*: Abrahams (1955), *AG*: Abrahams & Geller (1958), *BL*: Busing & Levy (1959, 1962) full matrix, *BP*: Batt & Post (1962), *EB*: this paper, *G*: Geller (1961), *GG*1 and *GG*2: Geller & Gilleo (1957, 1959), *P*: Prince (1957), *S*: Sayre, IBM, diagonal terms, *W*: Weidenborner (1961), *ZZ*: Zemann & Zemann (1961). Asterisks indicate refinements undertaken to produce relevant structure data; the others were listed to show the effects of different weight systems, matrix abbreviation, species and number of reflections, correlation of parameters (*e.g.*, s and B_h).

M	R	-10^4x	10^4y	10^4z	10^2B_h	10^2s	n_r	n_{ro}	F_o	w	LS	par	
Al,Si	Ca	389±5	456±5	1524±5	188±10		100	37	AG	AG	S	AG	*
		386 5	456 5	1522 5	179 10		"	"	"	GG1	"	"	
		391 4	456 4	1525 4	198 9		"	"	"	A	"	"	
		383 5	461 5	1521 5	134 15	96±3	"	"	"	GG1	BL	G	
		387 4	454 4	1510 4	144 12	97 2	88	"	"	"	"	"	
		381 7	458 6	1518 7	110 20	89 3	37	37	"	"	"	"	*
		388 4	458 4	1527 5	65 14	81 2	"	"	"	EB	"	EB	*
		388 4	456 4	1528 5	69 14	82 2	26	26	"	"	"	"	
		389 4	454 5	1528 5	74 17	82 2	21	21	"	"	"	"	
Al,Si	Mg	340 10	500 10	1540 10	40		108		ZZ	2-dim. refinement			*
Al	Y	290	530	1510			10		P	neutron diffraction			*
Fe	Y	274 9	572 9	1492 9	119	100	74	27	GG2	GG1	S	GG2	*
		279 6	591 6	1522 7	150 16	98 3	27	27	"	EB	BL	EB	
		279 6	590 6	1527 7	125f	94 1	"	"	"	"	"	"	
		280 6	589 7	1531 7	100f	91 1	"	"	"	"	"	"	
		280 8	588 8	1536 8	75f	87 1	"	"	"	"	"	"	
		280 9	587 10	1541 10	50f	84 2	"	"	"	"	"	"	
		264 6	569 9	1499 9	150f	102 2	24	24	EB	"	"	"	
		266 5	569 7	1501 7	125f	99 1	"	"	"	"	"	"	
		268 4	569 6	1503 6	100f	95 1	"	"	"	"	"	"	
		269 1	581 3	1495 1			17	17	BP	intensity ratios			*
Fe	Gd	286	534	1471	158		75	27	W	W	S	W	
		269 7	550 5	1478 5	132f	100f	"	"	"	"	BL	"	*
		274 9	547 7	1477 7	132 42	100 3	27	27	"	"	"	"	
		277 9	558 8	1495 9	173 25	101 4	"	"	"	EB	"	EB	*
		267 9	559 9	1493 9	132f	100f	"	"	"	"	"	"	

substantially lower r and significant changes in x, y, and z with YGaG, of z only with GdAlG and SmIG, and minor changes with the others.

The oxygen temperature factors B_h are mathematically coupled to the scale factors s as shown by Geller (1961) and demonstrated here by the correlation matrices (Table 3) which indicate also weak interdependence between the following parameters in descending order of importance: (s, z); (x, B_h); (s, x); (z, B_h); (x, y) and (y, z).

The structure data resulting from our refinements are shown in Table 4, and the relevant literature data for comparison in Table 5. With grossularite, the effects of weighting systems were insignificant, according to Abrahams & Geller (1958). Geller (1961) demonstrated the effects of matrix abbreviation (high B_h with diagonal terms *vs* full matrix), of excluding 12 reflections with poorly fitting F_o and of omitting all reflections with cation contributions (low B_h). To test our procedures, we repeated the least-squares refinement with their F_o and our weighting system, resulting in very low B_h, low s and somewhat high z. To simulate the situation encountered in the rare-earth garnets, we reduced the number of reflections with only minor changes in the resulting parameters.

The data on pyrope, $Al_2Si_3Mg_3O_{12}$, resulting from two-dimensional refinement by Zemann & Zemann (1961), compare reasonably well with our mineral sample (composition between that of pyrope and almandite $Al_2Si_3Fe_3O_{12}$).

Prince's (1957) parameters on YAlG appear to be somewhat different from ours, but their limits of error cannot be ascertained.

On YIG, a comparison of our x, y, and z with those obtained by Geller & Gilleo (1959) and Batt & Post (1962) shows differences which are mainly due to the use of three different sets of reflections. This became evident when we repeated the refinement with Geller & Gilleo's 27 'oxygen-only' reflections alone. Only 20

of these were included with our own sample, with 7 unobserved. Batt & Post's set of reflections is even more different as they used only those that appeared in pairs with common $h^2+k^2+l^2$. By forming intensity ratios within these pairs, they restricted the available input information further (equivalent to 9 observations) and compensated by reducing the number of refined variables (only x, y, and z) and by utmost precision of the measurements. The benefit from the latter is limited by such factors as the anisotropic thermal motion of the oxygen ions.

Even more sensitive to different sets of reflections are B_h and s. How these affect each other and also x and z is shown by a number of refinements in which B_h was kept fixed. With the data of Geller & Gilleo, only z changes significantly, while with ours both x and z change.

When the two sets of F_o are compared, our figures appear to be generally higher. However, on a basis of $s=1$, only $F_o(819)$ and $F_o(835)$ are different (of all 13 actually measured reflections common to both sets), which would probably have reduced $|F_o-F_c|$ in the Geller & Gilleo set.

With GdIG, Weidenborner (1961) found that the full matrix had to be used in the least-squares refinement. He determined B_h and s from the 'oxygen-only' reflections alone, B_{Gd} and B_{Fe} from reflections with strong cation contributions, and kept these parameters fixed when refining x, y, and z from all 75 reflections with predominant oxygen contributions. When we repeated the refinement with his oxygen-only reflections, B_h, z and y came out high, even when we kept B_h and s fixed.

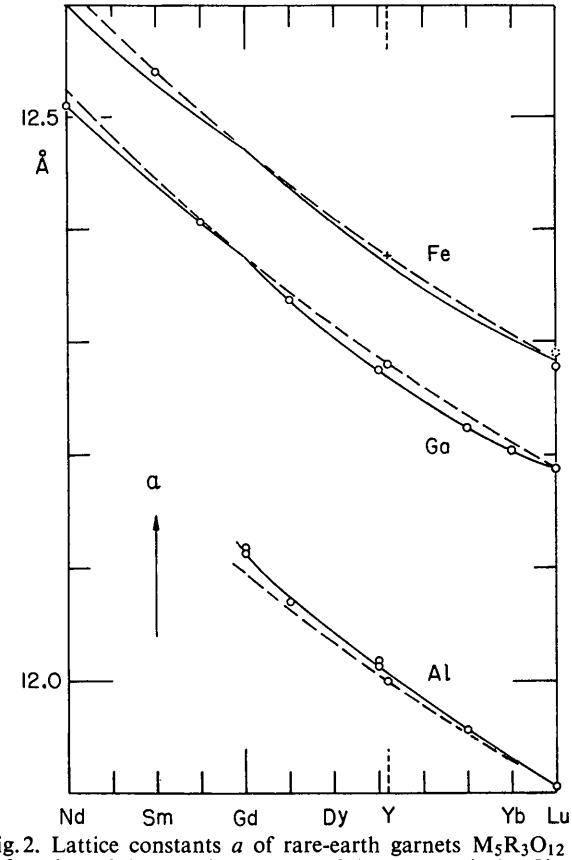

Fig. 2. Lattice constants a of rare-earth garnets $M_5R_3O_{12}$ as function of the atomic numbers of the rare earths R. Circles indicate our measurements. The data on the Fe series were taken from Espinosa (1962) with YIG fitted to the broken curve for spherical electron configurations of R.

In summary, our refinement procedure yields generally low B_h when compared with the literature. The figures for F_o fall into a common pattern for all our samples, but appear to be high, indicating low scale factors (by about 10%). These low B_h and s are causally connected as shown by high positive $a(s, B_h)$ in Table 3. They are also tied to more or less high z by the sizable negative $a(s, z)$ and $a(z, B_h)$ (except for the mineral sample). Judging from the other matrix elements, our x might be somewhat low while y should be hardly affected at all. These discrepancies tend to show that some of our parameters may have been obtained from too few observed reflections.

Discussion

The anion polyhedra in garnet form two linear repetitive arrangements (chains): (1) alternating tetrahedra and dodecahedra (about (d) and (c) along [001]) with shared edges d_{48} and (2) octahedra (about (a) along [111]). The latter chains are situated in {110} and {112} planes which are the predominant crystal faces. Around the point of closest approach between adjacent chains, the dodecahedra are situated. As a consequence, tetrahedra are formed between two neighboring dodecahedra.

The latter allow two different cation-anion distances d_8 and d_{80}. For $d_8=d_{80}$, they would degenerate into twisted prisms with rectangular bases parallel to {110}. Further degeneration would result in square bases, if $d_{88}=d_{68}$. The tetrahedra are always stretched along [001], since regular tetrahedra would require $d_4>d_6$, violating the rule that smaller cations have fewer nearest neighbors.

Adjacent polyhedra share three of the six anion–anion distances which are shortened, according to Pauling's rule: (1) $d_{48}<d_{41}$, which is necessary also to have $d_4<d_6$; (2) $d_{48}<d_{81}$, which makes $d_{80}<d_8$ and $\varphi>0$; (3) $d_{68}<d_{61}$ which causes $\sigma<\sigma_0$ (except in grossularite where Pauling's rule is less effective owing to the strong contribution of covalency in the binding).

When Espinosa (1962) plotted a of the Fe garnets *vs* the atomic number Z_R of the rare-earth elements R, he found a double festoon curve, caused by crystal field effects on the non-spherical R ions.

The same kind of effect is associated with the other two series as shown by the shape of the solid curves in Fig. 2. The magnitude of these effects appears to be different in the Fe and Ga series, indicated by the different spacings Δa between the solid and broken curves. The latter pertain to spherical R (Lu, Y, and Gd) and are parellel, *i.e.* the increments in a arising

from changes of M and R in $M_5R_3O_{12}$ are independent of each other. With the Al series, the broken line drawn parallel to the others pertains only to Lu and Y but not to the other rare-earth ions. Apparently, the higher electron density of the latter resists the compression imposed by the small lattice of the Al-garnets and necessitates an additional increase of a with increasing size of R. This makes it difficult to estimate the magnitude of the field effects due to non-spherical R which in this series is not represented by the spacing between the solid and broken curves. A 'spherical rare-earth curve' drawn through GdAlG and LuAlG might or might not have the same curvature as the broken line. Judging from the shape of the solid curve, however, the field effects cause a to decrease as in the other two series.

These details in a should also appear with the interionic distances and angles involved in the following equations:

$$a^2/16 = d_2^4 + d_{80}^2 - 2d_4 d_{80} \cos\alpha\,, \qquad (4)$$

$$\sqrt{3}a/4 = 2d_6 \cos\sigma \cos\varphi' + d_{88} \cos\varphi''\,, \qquad (5)$$

α being the bond angle (d)–(h)–(d_{80})–(c), $\varphi' = \varphi/\sin\sigma$ and $\varphi'' = \varphi' d_{88}/2d_6$. The broken lines in Figs. 3 and 4 show how the additivity of a is associated with additive distances and angles fitted to the observations within error limits (except φ which plays merely a minor role here because of its small size and the cosine function).

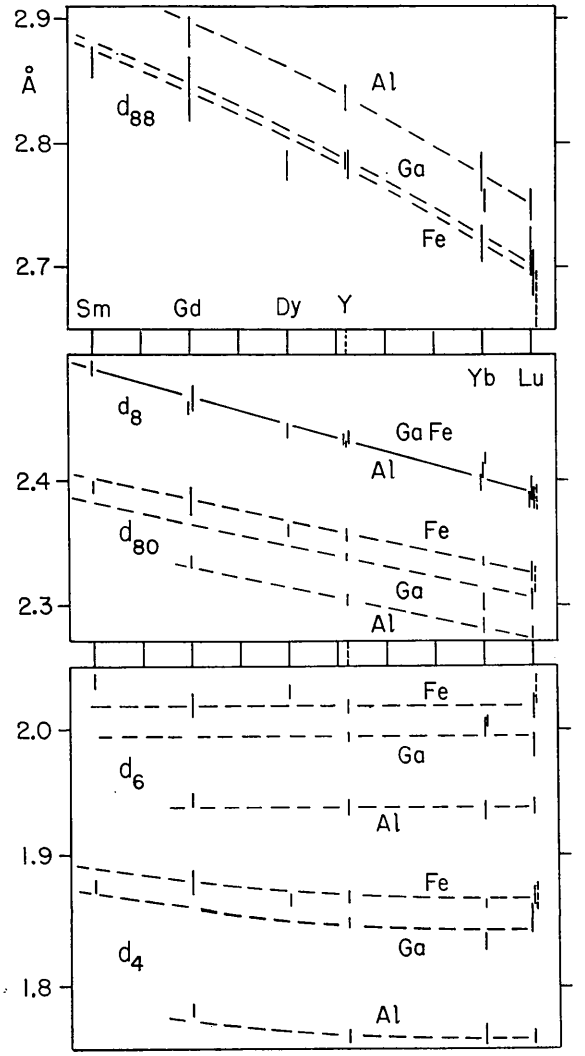

Fig. 3. Selected interionic distances in rare-earth garnets $M_5R_3O_{12}$ as function of the atomic numbers of the rare earths R. The place of Y and the broken curves, pertaining to spherical R, correspond to Fig. 2. Where data fall close together, M reads from left to right: Al, Ga, Fe. The broken vertical lines relate to LuIG sample *M*. The data on GdIG are based on our refinement of s, x, y, z and B_h with Weidenborner's (1961) F_o.

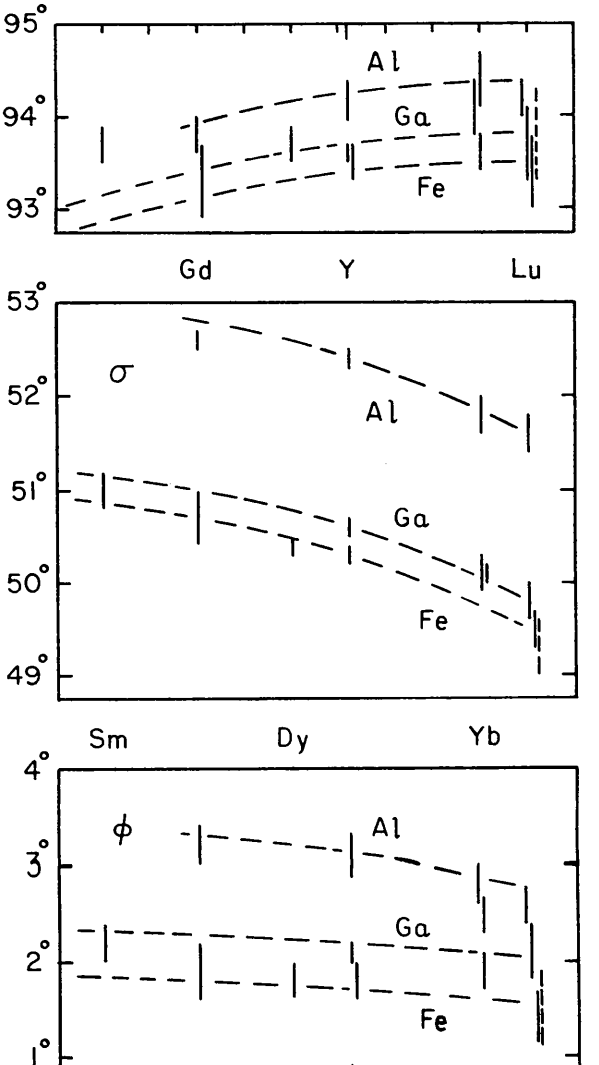

Fig. 4. Bond angle (d)-(h)-(d_{80})-(c), 'cone angle' σ and azimuth φ of vector **p** in rare-earth garnets $M_5R_3O_{12}$ as function of the atomic numbers of the rare earths R. For details see legend of Fig. 3.

In addition, the field effects on non-spherical ions seem to show up with d_{80}, d_4, d_{88} and d_6 (the latter with changed sign) of SmIG and DyIG. With LuIG sample M*, their appearance is probably due to non-spherical rare-earth impurities. These would explain also the high a and the change of sign in the magnetic anisotropy found by Czerlinsky & Field (1960) with this sample. In contrast, sample B shows the expected anisotropy equal to that of YIG according to Gianino and Czerlinsky (1963).

The low a of the latter sample lies within error limits, while the high a of SmIG indicates the presence of larger ions. Our a was obtained from flux-grown crystals, Espinosa's from pure sintered material. Therefore, the magnitude of the field effects on a in the different garnet series cannot be compared quantitatively.

The distance d_8 is apparently independent of M, at least for spherical R. Of the non-spherical R, only Yb is available in all three series with significant dependence of d_8 on M. YbIG shows small d_6 and large d_{88} and d_8 which would indicate exceptionally strong rigidity of Yb in that case.

The rigidity effect observed on a in the Al series appears also with all the distances and angles shown in Figs. 3 and 4. The small lattice calls for a large decrease of d_{80} which is resisted by the rigidity of the rare-earth ions so that d_{80} is actually larger than required for additivity. Two causal chains start from here:

(1) The shared edge d_{48} is enlarged (meaning smaller α), the positive charge between (c) and (d) decreased, and consequently, d_4 increased.
(2) The total lattice responds by squeezing d_8 and d_{88}, associated with increased d_6. Consequently, the shared edge d_{68} decreases (smaller σ), and the increased positive charge between (c) and (a) reduces the increase of d_6. The effect is apparently characterized by equal differences d_8–d_{80} in Lu Al G and Gd Al G.

It can be shown that φ is proportional to the distortion of the tetrahedra and dodecahedra, while the shape of the octahedra is independent of φ. The difference $\sigma_0-\sigma$, however, is proportional to the distortion of the octahedra and tetrahedra, while its influence upon the dodecahedra is more complicated. The relationship between σ and φ shown in Fig. 5 is a result of these effects, a compromise between minimum distortion and shortened shared edges of the polyhedra.

The magnetic g-tensors of trivalent Nd, Dy, Er and Yb have been observed in Y, Lu, Tm, Ga and Al host garnets by Boakes, Garton, Ryan & Wolf (1959), Carson & White (1960), Wolf, Ball, Hutchings, Leask & Wyatt (1961), and Hutchings & Wolf (1963). When the components of g in the directions [$\bar{1}$01], [101] and [010] are plotted *vs* φ obtained from the broken lines in Fig. 4, the extrapolated curves meet at $\varphi\sim1{\cdot}5°$ with $g\sim3{\cdot}4$ for Yb and $g\sim2{\cdot}5$ for Nd. Such conditions for isotropic g do not exist for Dy and Er.

It has been shown in Figs. 2, 3 and 4 that cell edges, interionic distances and angles in garnets can be interpreted by a consistent system within error limits. Although this system probably shows correct trends within itself, it may be in need of adjustment to agree with the literature data. With YIG and GdIG, our refinement resulted in lower d_4 and higher d_6, while d_4 in LuGaG and YGaG appears to be high against the average tetrahedral Ga–O distance of 1·83 Å found in β-Ga_2O_3 by Geller (1960).

The authors wish to thank their colleagues Drs P. Gielisse and N. Yannoni and J. Silverman for most valuable help and discussions; Drs C. Pitha, G. Garton, R. Lefever, P. C. Bailey and Mr J. J. Moriarty for providing the crystals; Messrs J. J. Fitzgerald, J. J. O'Connor and J. Weiner for the chemical analysis of the mineral sample. Finally, they acknowledge most gratefully the extensive efforts of Dr E. R. Czerlinsky who originally started this work and supported it with continued active interest.

* Preliminary x, y, z published earlier by Czerlinsky & Euler (1961) were determined on this sample.

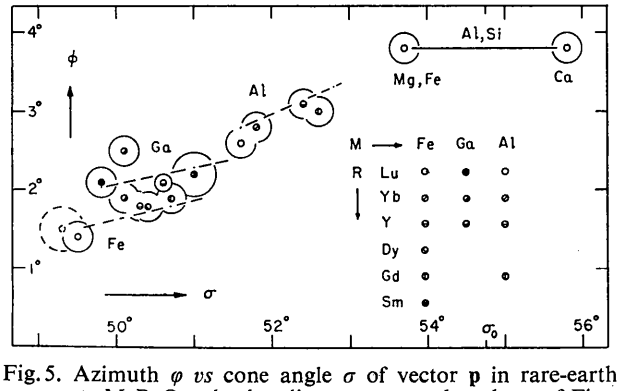

Fig. 5. Azimuth φ *vs* cone angle σ of vector **p** in rare-earth garnets $M_5R_3O_{12}$; broken lines correspond to those of Figs. 2, 3 and 4.

References

ABRAHAMS, S. C. (1955). *Acta Cryst.* **8**, 661.
ABRAHAMS, S. C. & GELLER, S. (1958). *Acta Cryst.* **11**, 437.
BATT, A. & POST, B. (1962). *Acta Cryst.* **15**, 1268.
BOAKES, D., GARTON, G., RYAN, D. & WOLF, W. P. (1959). *Proc. Phys. Soc. Lond.* **76**, 663.
BOND, W. L. (1951). *Rev. Sci. Instrum.* **22**, 344.
BOND, W. L. (1959). *Acta Cryst.* **12**, 375.
BUSING, W. R. & LEVY, H. A. (1959). *A Crystallographic Least Squares Refinement Program for the IBM* 704, Oak Ridge: Oak Ridge National Laboratories. Central Files No. 59-4-37.
BUSING, W. R., MARTIN, K. O. & LEVY, H. A. (1962). *ORFLS Fortran Crystallographic Least Squares Program (for IBM* 7090). Oak Ridge National Laboratories, ORNL-TM-305.
BUSING W. R., MARTIN, K. O. & LEVY, H. A. (1964). *ORFFE Fortran Crystallographic Function and Error Program.* ORNL-TM-306.

CARSON, J. W. & WHITE, R. L. (1960). *J. Appl. Phys.* **31**, 53S.
CZERLINSKY, E. R. & EULER, F. (1961). *Rare Earth Research.* p. 113. New York: Macmillan.
CZERLINSKY, E. R. & FIELD, W. G. (1960). *Solid State Physics in Electronics and Telecommunications.* Vol. 3, p. 488. New York: Academic Press.
ESPINOSA, G. P. (1962). *J. Chem. Phys.* **37**, 2344.
FREEMAN, A. J. (1959). *Acta Cryst.* **12**, 261.
GELLER, S. & GILLEO, M. A. (1957). *Phys. Chem. Solids*, **3**, 30.
GELLER, S. & GILLEO, M. A. (1959). *Phys. Chem. Solids*, **9**, 235.
GELLER, S. (1960). *J. Chem. Phys.* **33**, 676.
GELLER, S. (1961). *Acta Cryst.* **14**, 1026.
GIANINO, P. & CZERLINSKY, E. R. (1963). *Bull. Amer. Phys. Soc.* **8**, 144, B4.
HUTCHINGS, M. T. & WOLF, W. P. (1963). *Phys. Rev. Letters*, **11**, 187.
International Tables for X-ray Crystallography (1952). Vol. I, p. 345. Birmingham: Kynoch Press.
MENZER, G. (1928). *Z. Kristallogr.* **69**, 300.
PAULING, L. (1960). *The Nature of the Chemical Bond.* 3rd. ed., p. 561. Ithaca: Cornell Univ. Press.
PRINCE, E. (1957). *Acta Cryst.* **10**, 787.
RENNINGER, M. (1937). *Z. Physik*, **106**, 141.
TUNELL, G. (1939). *Amer. Min.* **24**, 448.
WEIDENBORNER, J. E. (1961). *Acta Cryst.* **14**, 1051.
WOLF, W. P., BALL, M., HUTCHINGS, M. T., LEASK, M. J. M. & WYATT, A. F. G. (1961). *J. Phys. Soc. Japan*, **17**, BI, 443.
YAKEL, H. L. & FANKUCHEN, I. (1962). *Acta Cryst.* **15**, 1188.
ZEMANN, A. & ZEMANN, J. (1961). *Acta Cryst.* **14**, 835.

Acta Cryst. (1965). **19**, 978

The Crystal and Molecular Structure of Allylthiourea

BY K. S. DRAGONETTE AND I. L. KARLE
U.S. Naval Research Laboratory, Washington, D.C., U.S.A.

(*Received* 22 *March* 1965)

The crystal structure of allylthiourea has been determined by direct phase determination employing the symbolic addition procedure. The space group is $P2_1/c$ with the following cell parameters: $a=8{\cdot}39$ Å, $b=8{\cdot}58$ Å, $c=9{\cdot}77$ Å, $\beta=119°\ 45'$, and $Z=4$. A three-dimensional least-squares refinement with anisotropic temperature factors for the C, N and S atoms was performed. All the hydrogen atoms were located from a difference Fourier map. Hydrogen bonds between the sulfur and nitrogen atoms link the molecules in a continuous chain parallel to the b axis. The S · · · H–N bonds are 3·36 Å. The thiourea group is planar and the C=S bond is 1·66 Å, a value somewhat smaller than that found in thiourea and some of its derivatives.

Introduction

The structures of thiourea (Kunchur & Truter, 1958) and a number of its derivatives such as thioacetamide (Truter, 1960), trimethylenethiourea (Dias & Truter, 1964) and ethylenethiourea (Wheatley, 1953) have been carefully determined in a program to study the C=S bond. The investigation of allylthiourea,

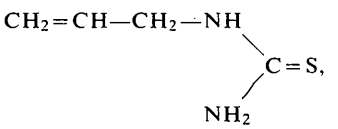

was undertaken for the purpose of comparing bond lengths and angles and the mode of possible hydrogen bonding between the sulfur and nitrogen atoms with the structures already determined.

Experimental

Crystals of allylthiourea form white plates elongated parallel to the b axis. Unit-cell parameters were determined from precession photographs with the crystal mounted on the b axis and using copper radiation. They are

$$a=8{\cdot}39\pm0{\cdot}02,\quad b=8{\cdot}58\pm0{\cdot}01,\quad c=9{\cdot}77\pm0{\cdot}01\ \text{Å}$$
$$\beta=119°45'\pm10',\quad Z=4\,.$$

The calculated density is 1·264 g.cm^{-3}; the measured density was found to be 1·247 g.cm^{-3} by the flotation method employing mixed solvents. The present analysis is in agreement with the crystallographic information published previously for allylthiourea (Whitney & Corvin, 1949).

Intensity data were obtained from multiple film, equi-inclination Weissenberg photographs. The rotation axis was parallel to the b axis and layers 0 through 6 were collected. Extinctions indicated that the space group was $P2_1/c$.

Intensities from the Weissenberg photographs were estimated visually by comparison with a calibrated film strip. Corrections for spot size, and Lorentz and polarization factors were computed with a revision by Mr Stephen Brenner of an earlier data reduction program (Norment, 1962) for the IBM 7030 (STRETCH) computer. No absorption corrections were made. The data